

## Positive and negative couplings perform complementary roles in the signal amplification of globally coupled bistable oscillators

Xiaoming Liang <sup>1,\*</sup>, Cong Liu <sup>1</sup> and Xiyun Zhang<sup>2</sup>

<sup>1</sup>*School of Physics and Electronic Engineering, Jiangsu Normal University, Xuzhou 221116, China*

<sup>2</sup>*Department of Physics, Jinan University, Guangzhou, Guangdong 510632, China*



(Received 4 November 2019; revised manuscript received 28 December 2019; accepted 27 January 2020; published 10 February 2020)

We investigate a system of globally coupled bistable oscillators subjected to a common weak signal, where the couplings are oscillator dependent with random signs: positive or negative. We find that neither purely positive nor purely negative couplings are optimal for signal amplification of the system; a mixture of both positive and negative couplings is more beneficial for the signal amplification. Our numerical results further show that different from the fully synchronous state caused by purely positive couplings or asynchronous state caused by purely negative couplings, the mixed positive and negative couplings can generate a clustering synchronous state, which allows the system to generate a resonancelike response to the weak signal, and thus, amplifies the signal. We finally propose a reduced model to analyze the mechanism underlying this resonancelike behavior, and find a complementary effect of these two types of couplings in signal amplification.

DOI: [10.1103/PhysRevE.101.022205](https://doi.org/10.1103/PhysRevE.101.022205)

### I. INTRODUCTION

Understanding the collective response of nonlinear systems consisting of large numbers of coupled oscillators to external weak inputs is of great interest in science and technology [1–6]. Since natural systems are undeniably subject to noisy fluctuations, large efforts have been made to understand the role of randomness in weak signal amplification [7,8]. Stochastic resonance (SR) is a classic example of nontrivial effect of randomness on signal amplification, wherein the response of a nonlinear system to a weak signal is significantly increased by the presence of a particular level of noise [9,10]. Moreover, the SR effect can be optimized by an intermediate number of interacting units, i.e., system size resonance [11–13].

Another typical example of the randomness-enhanced signal amplification is diversity-induced resonance [14–17]. Different from external noise, diversity denotes the statically stochastic differences among the units of the systems, which comes from the intrinsic different properties for each unit [8,18]. Similar to noise, diversity can induce a resonant collective response in an ensemble of coupled bistable or excitable units [14]. Besides the diversity of the units, systems' randomness can be from the heterogeneity in their coupling strength and interaction network topologies [19–23], and the randomness also affects the performance of signal amplification. For instance, in contrast to regular arrays, complex topologies such as small-world and scale-free networks may generate a stronger SR effect [24–27]. Owing to weighted couplings, ensembles of bistable oscillators can display a higher response

to a weak external signal, compared to that of the unweighted counterparts [28–31].

In the majority of studies on signal amplification, the couplings among units are set to be positive (excitatory). However, negative (inhibitory) couplings are very common in biological systems [32–38]. For example, in small-scale brain areas suffering from incurable epilepsy, the interaction between neighboring astrocytes is phase repulsive and is stronger than that of the normal astrocyte cultures [39]. In large-scale brain networks, there are two types of neurons, excitatory and inhibitory, and an approximate ratio of 70% excitatory and 30% inhibitory neurons is crucial for healthy brain activity [40]. Moreover, the competition between positive and negative couplings plays an important role in cognitive function [40,41]. Thus, it is interesting to investigate the role of randomness of coupling types on signal amplification.

In the present work, motivated by neural networks with excitatory and inhibitory neurons, we study a system of globally coupled bistable oscillators subjected to a common weak signal, where the couplings are oscillator dependent with random signs: positive or negative. The bistable oscillators with positive couplings can be considered as “excitatory neurons” as in neural networks, which tend to fall in line with other units. While the bistable oscillators with negative couplings are “inhibitory neurons,” which tend to repel the other units. Compared with the conventionally purely positive or negative coupled systems, we find that our system with mixed positive and negative couplings can show a larger signal amplification. Moreover, we find that the coupling strength as well as the ratio between the two types of couplings jointly adjust the enhancement of signal amplification. Further, we use a reduced model to reveal the cooperation between the two types of couplings in signal amplification.

\*xmliang@jsnu.edu.cn

## II. MODEL

We consider a system of globally coupled bistable oscillators; the dynamics are governed by

$$\dot{x}_i = x_i - x_i^3 + \frac{k_i}{N} \sum_{j=1}^N (x_j - x_i) + A \sin(\omega t), \quad i = 1, \dots, N, \quad (1)$$

where  $k_i$  can be positive or negative representing the coupling strength of the  $i$ th oscillator.  $k_i > 0$  means the  $i$ th oscillator tends to follow other oscillators which promotes global synchrony, while oscillators with  $k_i < 0$  tend to repel the others which suppress the global synchrony. Specifically, we randomly assign the value of  $k_i$  with

$$k_i = \begin{cases} -K, & \text{with probability } p, \\ K, & \text{with probability } 1 - p, \end{cases}$$

where  $K \geq 0$ . The couplings are purely positive when  $p = 0$ , while for  $p = 1$  the couplings are purely negative. Thus, the intermediate values of  $p$  correspond to the case of mixed positive and negative couplings.

A  $\sin(\omega t)$  denotes the external signal with amplitude  $A$  and frequency  $\omega$ . For an isolated bistable oscillator, i.e.,  $k_i = 0$ , the threshold for the amplitude of the external signal to generate an amplified output signal is  $A_c = 2/\sqrt{27} \approx 0.38$  [9]. For a weak external signal with  $A < A_c$ , the bistable oscillator will jiggle around one of its two stable fixed points  $x_s = \pm 1$ ; while for a strong external signal with  $A > A_c$ , the bistable oscillator can jump between the two stable fixed points with a large amplitude. In our simulation, we consider a weak external signal by setting  $\omega = \pi/50$  and  $A = 0.2$ .

A convenient way to measure the system's response to the external signal is to use the signal amplification factor  $G$  defined as [26]

$$G = \frac{\max_t X(t) - \min_t X(t)}{2A}, \quad (2)$$

where  $X(t) = N^{-1} \sum_{i=1}^N x_i(t)$  stands for the average activity of the system. When the oscillators behave disordered,  $X(t)$  fluctuates with small amplitudes leading to a small  $G$ . Instead,  $G$  is large when the oscillators behave coherently with large amplitudes. In our numerical simulations, we consider  $N = 1000$  bistable oscillators in system (1) and randomly choose their initial conditions from the two fixed points  $x_s = \pm 1$ . Moreover, we calculate the averaged amplification  $\langle G \rangle$  over 1000 realization with different initial conditions.

## III. NUMERICAL RESULTS

We start from the case of purely positive coupling, i.e.,  $p = 0$ . We find that the average amplification  $\langle G \rangle$  keeps increasing with  $K$  until a critical value of  $K_1 = 0.24$ , and then drops discontinuously to the value as at  $K = 0$  forming a coupling-induced resonance [see Fig. 1(a)]. Time series of oscillators show that for  $K < K_1$  the system splits into two oscillation clusters centered around  $x_s = \pm 1$  separately [see Fig. 1(b)], while for  $K > K_1$  the system forms a fully synchronous cluster behaving like a single oscillator as for  $K = 0$  [see Fig. 1(c)], and this transition from cluster synchronization to full synchronization leads to the observed coupling-induced

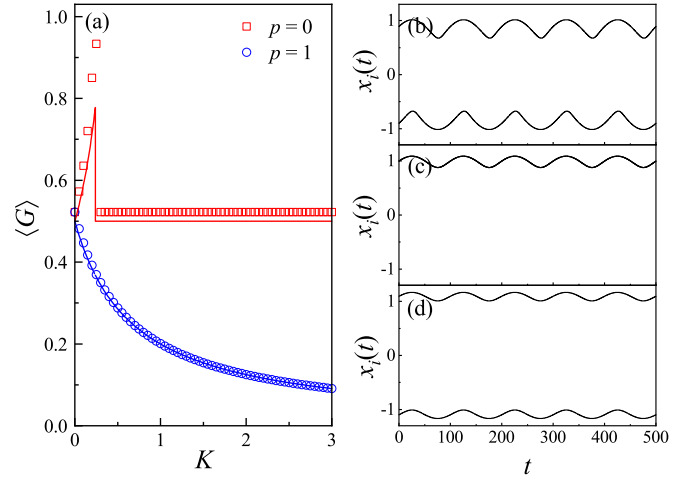


FIG. 1. (a) Average amplification  $\langle G \rangle$  of Eq. (1) versus  $K$  for  $p = 0$  and 1. Solid lines denote the theoretical results of Eqs. (11), (19), and (43). Time series of Eq. (1) with  $p = 0$  and  $K = 0.2$  in (b),  $p = 0$  and  $K = 0.4$  in (c), and  $p = 1$  and  $K = 0.2$  in (d).

resonance. In the case of purely negative couplings, i.e.,  $p = 1$ , the average amplification  $\langle G \rangle$  decreases monotonously with increase of  $K$ , showing a damped response [see Fig. 1(a)]. Time series of oscillators show that two oscillation clusters keep away from each other [see Fig. 1(d)], leading to the decline in the response. These two distinct responses indicate that intermediate degrees of synchronization with small positive couplings may promote the signal amplification; in contrast, neither full synchronization with large positive couplings nor desynchronization with purely negative couplings is beneficial for amplifying a weak external signal.

Next, we turn to the case of mixed positive and negative couplings, i.e.,  $0 < p < 1$ . We find that for a small  $p$ , e.g.,  $p = 0.3$ , the average amplification  $\langle G \rangle$  exhibits a double resonance with two peaks at  $K_1 = 0.24$  and  $K_2 = 1.4$  [see Fig. 2(a)]. As  $p$  increases to  $p = 0.5$ , the two resonance peaks decrease

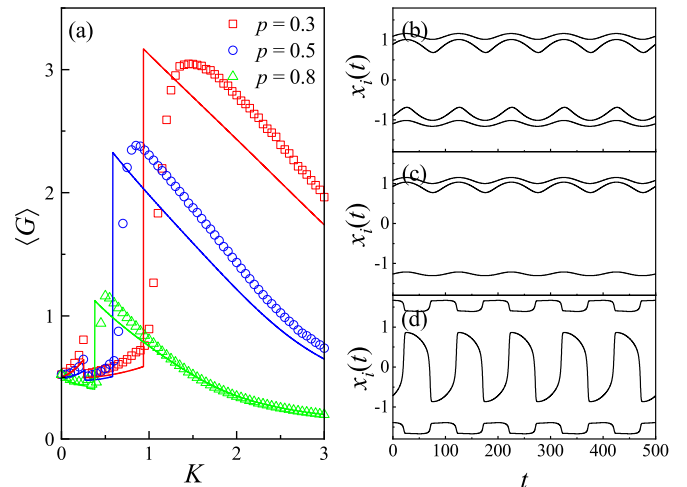


FIG. 2. (a) Average amplification  $\langle G \rangle$  of Eq. (1) versus  $K$  for  $p = 0.3, 0.5$ , and  $0.8$ . Solid lines denote the theoretical results of Eq. (43). Time series of Eq. (1) for  $p = 0.3$  with (b)  $K = 0.2$ , (c)  $K = 0.4$ , and (d)  $K = 1.4$ .

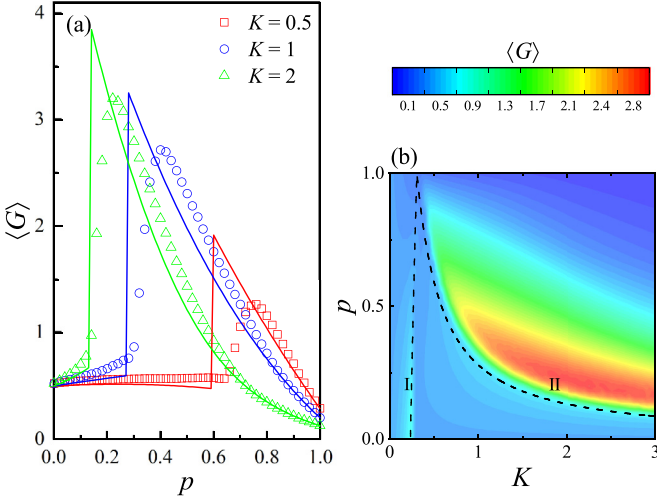


FIG. 3. (a) Average amplification  $\langle G \rangle$  of Eq. (1) versus  $p$  for  $K = 0.5, 1$ , and  $2$ . Solid lines denote the theoretical results of Eq. (43). (b) The dependence of  $\langle G \rangle$  on both the  $K$  and  $p$ . Dashed lines denote the theoretical results of Eqs. (31) and (36).

their heights, where  $K_1$  corresponding to the first peak stays unchanged while  $K_2$  corresponding to the second peak shifts towards  $K_1$ . With further increase of  $p$ , e.g.,  $p = 0.8$ , the first peak at  $K_1$  disappears leaving only the second peak with a small height at  $K_2 = 0.5$ . Compared to the cases of purely positive and purely negative couplings, a mixture of both types of couplings shows an advantage in amplifying weak signals with a much higher amplification factor  $\langle G \rangle$ , especially for relatively smaller  $p$ . To understand the occurrence of observed double resonance, we show the time series of Eq. (1) at  $p = 0.3$  for three different  $K$  in Figs. 2(b)–2(d). For a small  $K = 0.2$  below  $K_1$ , the system exhibits four oscillation clusters resembling the superposition of the states of  $p = 0$  and  $p = 1$  [see Fig. 2(b)]. For an intermediate  $K = 0.4$  in between the two resonance peaks, the two clusters in the middle merge into one cluster similar to the case of  $p = 0$  [see Fig. 2(c)]. While for a large  $K = 1.4$  above the second resonance peak, the middle cluster oscillates with a large amplitude between the other two clusters [see Fig. 2(d)]. These observations indicate that three oscillation clusters induced by the mixed two types of couplings is the origin of the secondary resonance at  $K_2$ , which leads to the enhancement of signal amplification.

In Fig. 3(a), we show the average amplification  $\langle G \rangle$  varies with the probability  $p$  for different  $K$ . Compared to the cases of  $p = 0$  and  $p = 1$ , a mixture of positive and negative couplings, i.e.,  $0 < p < 1$ , can significantly amplify the weak signal exhibiting a resonant dependence on  $p$ . With  $K$  increases the resonance effect becomes more and more pronounced, while the optimal  $p$  for the resonance peak decreases. Figure 3(b) further shows the average amplification  $\langle G \rangle$  on the  $(K, p)$  plane. The amplified signal response can be observed in two regions: region I and region II corresponding to the two resonance phenomena in Fig. 2(a), respectively. In contrast, region II has a larger space and higher response than that of region I. Moreover,  $p$  and  $K$  for the boundary of region II approximately follows  $p \propto K^{-1}$  meaning that for a large

coupling strength  $K$ , only a small probability  $p$  is needed to optimize the system's ability for signal amplification.

#### IV. ANALYTICAL RESULTS

According to numerical results shown in Fig. 1, purely repulsive couplings cannot amplify weak signals, and purely positive couplings can enhance signal amplification only for small coupling strength. Interestingly, a mixture of both positive and negative couplings can eliminate the disadvantageous effects of these two pure couplings, and improve the system's ability to amplify the weak external signal [see Fig. 2]. One hypothesis for the underlying mechanism of this observation is the existence of the following process: (i) The oscillators with negative couplings split into two clusters fluctuating around two stable fixed points  $x_s = \pm 1$  separately due to their repulsive interactions; (ii) oscillators with positive couplings form the third cluster tending to merge with the other clusters due to its attractive interaction; (iii) when the third cluster with positive couplings approaches one of the repulsive clusters, the attraction between them becomes weaker because of the decrease in coupling effect  $k_i(x_j - x_i)$  [defined in Eq. (1)]; (iv) meanwhile the attraction between the attractive cluster with the other repulsive cluster (which is far away) becomes stronger and turns the attractive cluster back; (v) the repeated cycle of (iii) and (iv) makes the attractive cluster oscillate between the two repulsive clusters with a large amplitude. This process describes the complementary roles of the positive and negative couplings in signal amplification. To test this hypothesis, we analyze the different coupling cases of our simulation.

##### A. Case I: $p = 0$

For purely positive couplings, the oscillators spontaneously split into two clusters according to their two different initial conditions. For simplicity, we assume the two clusters to be of the same size, i.e., half of the oscillators with positive initial conditions ( $x_i(0) = 1$ ) belonging to cluster A, and the other half with negative initial conditions ( $x_i(0) = -1$ ) belonging to cluster B. Due to the same initial conditions, the oscillators within each cluster behave identically. Defining  $y_1$  and  $y_2$  as the collective dynamics of cluster A and cluster B, Eq. (1) can be simplified into a two-oscillator system as

$$\begin{aligned} \dot{y}_1 &= y_1 - y_1^3 + \frac{K}{2}(y_2 - y_1) + A \sin(\omega t), \\ \dot{y}_2 &= y_2 - y_2^3 + \frac{K}{2}(y_1 - y_2) + A \sin(\omega t). \end{aligned} \quad (3)$$

Introducing  $Y = (y_1 + y_2)/2$  and  $Z = (y_1 - y_2)/2$  as the average activity and synchronization error of the two clusters, respectively, Eq. (3) can be further rewritten as

$$\dot{Y} = (1 - 3Z^2)Y - Y^3 + A \sin(\omega t), \quad (4)$$

$$\dot{Z} = (1 - K - 3Y^2)Z - Z^3. \quad (5)$$

Assuming  $Z$  relaxes much more rapidly than  $Y$ , one can perform an adiabatic elimination, i.e.,  $\dot{Z} = 0$ . From Eq. (5), we obtain  $Z^2 = 1 - K - 3Y^2$  and  $Z = 0$ , which correspond to

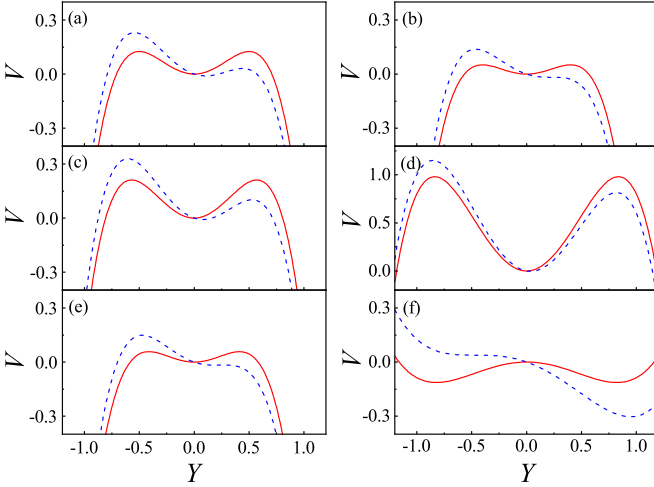


FIG. 4. (Upper panels) The potential of Eq. (7) for (a)  $K = 0$  and (b)  $K = 0.24$ . (Middle panels) The potential of Eq. (17) for (c)  $K = 0$  and (d)  $K = 0.4$ . (Lower panels) The potential of Eq. (30) for (e)  $K = 0.24$  and of Eq. (35) for (f)  $K = 0.95$ . Solid and dashed lines denote the potential at  $t = 0$  and  $t = \pi/2\omega$ , respectively.

desynchronization and full synchronization between cluster A and cluster B, respectively.

Considering the two clusters are out of synchronization, i.e.,  $Z^2 = 1 - K - 3Y^2$ , Eq. (4) becomes

$$\dot{Y} = (-2 + 3K)Y + 8Y^3 + A \sin(\omega t), \quad (6)$$

which describes the overdamped motion of a particle in a coupling-dependent potential with a periodic force. Adding the signal to the potential, we get

$$V = \frac{(2 - 3K)}{2}Y^2 - 2Y^4 - YA \sin(\omega t). \quad (7)$$

Since the signal amplitude  $A$  is fixed, the modulation of coupling strength  $K$  becomes important to the potential  $V$ . Figure 4 illustrates the dependence of  $V$  on  $K$ . For  $K = 0$ , the potential  $V$  is M shaped with a single well and two barriers on the sides. As  $t$  evolves, the two barriers periodically rise and fall but maintaining the well [see Fig. 4(a)]. In this case the particle cannot pass over the barriers if it is initially in the potential well. With  $K$  increases, e.g.,  $K = 0.24$ , the potential barriers vanish when the external signal arrives at its maximum or minimum, and the particle can pass over the barriers [see Fig. 4(b)]. For  $K > 0.24$  the external signal is suprathreshold which can force the particle out of the potential well, and thus,  $K_1 = 0.24$  is the critical coupling strength.

Since the external signal is subthreshold when  $K < K_1$ , one can solve Eq. (6) by linearization. The approximate solution is obtained as

$$Y(t) \approx \frac{A}{\sqrt{(2 - 3K)^2 + \omega^2}} \sin(\omega t + \phi_1), \quad (8)$$

where  $\phi_1$  is phase shift.

When  $K > K_1$ , the external signal is suprathreshold, which drives the two clusters into full synchronization, i.e.,  $Z = 0$ . Then Eq. (4) becomes

$$\dot{Y} = Y - Y^3 + A \sin(\omega t), \quad (9)$$

which is the isolated bistable oscillator subjected to a subthreshold signal, i.e., Eq. (1) at  $K = 0$ . Its solution is approximately given by

$$Y(t) \approx \pm 1 + \frac{A}{\sqrt{4 + \omega^2}} \sin(\omega t + \phi_2), \quad (10)$$

where  $\phi_2$  represents phase shift.

Inserting Eqs. (8) and (10) into Eq. (2), we obtain the theoretical amplification as

$$G \approx \begin{cases} \frac{1}{\sqrt{(2-3K)^2 + \omega^2}}, & \text{if } K < K_1, \\ \frac{1}{\sqrt{4 + \omega^2}}, & \text{if } K > K_1. \end{cases} \quad (11)$$

Equation (11) suggests that the system generates a maximum amplification near the boundary of full synchronization at  $K = K_1$ . The predicted amplification of Eq. (11) is in good agreement with the numerical result of Eq. (1) at  $p = 0$  [see Fig. 1(a)].

We now analyze the critical coupling strength  $K_1$  for full synchronization. As shown in Fig. 4(b), the potential  $V$  loses its stability at  $K = K_1$ . This corresponds to the condition that the cubic function  $(-2 + 3K)Y + 8Y^3 + A = 0$  has three roots with two equal, which results in

$$\left(\frac{A}{16}\right)^2 = \left(\frac{2 - 3K}{24}\right)^3. \quad (12)$$

For  $A = 0.2$ , the critical coupling strength is given by

$$K_c = \frac{2}{3} - (2A^2)^{\frac{1}{3}} \approx 0.24, \quad (13)$$

which is in good agreement with the numerical result  $K_1 = 0.24$ .

## B. Case II: $p = 1$

When  $p = 1$ , the oscillators also split into two clusters at  $t = 0$  according to their initial conditions. Different from  $p = 0$ , with  $t$  evolving, the two clusters cannot synchronize, but repel each other due to the purely negative couplings. Nevertheless, the oscillators within each cluster behave identically due to the same initial conditions. Using the same assumption and definition as used in  $p = 0$ , we arrive at the following equations:

$$\dot{Y} = (1 - 3Z^2)Y - Y^3 + A \sin(\omega t), \quad (14)$$

$$\dot{Z} = (1 + K - 3Y^2)Z - Z^3. \quad (15)$$

Similarly, we assume  $Z$  relaxes more rapidly than  $Y$  and thus can be adiabatically eliminated, i.e.,  $\dot{Z} = 0$ . This leads to  $Z^2 = 1 + K - 3Y^2$  and  $Z = 0$ . Since the two clusters are out of synchronization at  $p = 1$ , we substitute  $Z^2 = 1 + K - 3Y^2$  into Eq. (14) and get

$$\dot{Y} = -(2 + 3K)Y + 8Y^3 + A \sin(\omega t). \quad (16)$$

Analogously, the potential of Eq. (16) can be expressed as

$$V = \frac{(2 + 3K)}{2}Y^2 - 2Y^4 - YA \sin(\omega t). \quad (17)$$

Figures 4(c) and 4(d) show that the potential  $V$  of Eq. (17) is M shaped and its potential well gets deeper with the increase of  $K$ . As a result, the external signal remains subthreshold

and the dynamic range of the particle within the potential well becomes narrower when  $K$  increases. Using linearization, we can obtain the approximate solution of Eq. (16), which is given by

$$Y(t) \approx \frac{A}{\sqrt{(2+3K)^2 + \omega^2}} \sin(\omega t + \phi_3), \quad (18)$$

where  $\phi_3$  denotes the phase shift. Putting Eq. (18) into Eq. (2), we obtain the theoretical amplification as

$$G \approx \frac{1}{\sqrt{(2+3K)^2 + \omega^2}}. \quad (19)$$

Equation (19) suggests a damped amplification at  $p = 1$ , which coincides with the numerical result of Eq. (1) [see Fig. 1(a)].

### C. Case III: $0 < p < 1$

When  $0 < p < 1$ , the oscillators are initially divided into four clusters according to both the signs of the couplings and the initial conditions. For simplicity, we assume that  $pN/2$  oscillators are with  $x_i(0) = 1$  and  $k_i > 0$  belonging to cluster A,  $(1-p)N/2$  oscillators are with  $x_i(0) = 1$  and  $k_i < 0$  belonging to cluster B,  $pN/2$  oscillators are with  $x_i(0) = -1$  and  $k_i > 0$  belonging to cluster C, and  $(1-p)N/2$  oscillators are with  $x_i(0) = -1$  and  $k_i < 0$  belonging to cluster D. Let  $y_1, y_2, y_3,$  and  $y_4$  denote the collective dynamics of the four clusters; then Eq. (1) reduces to a four-oscillator system as

$$\begin{aligned} \dot{y}_1 &= \left[ 1 - \frac{K(1+p)}{2} \right] y_1 - y_1^3 \\ &\quad + K \left[ \frac{p}{2} y_2 + \frac{1-p}{2} y_3 + \frac{p}{2} y_4 \right] + A \sin(\omega t), \\ \dot{y}_2 &= \left[ 1 - \frac{K(p-2)}{2} \right] y_2 - y_2^3 \\ &\quad - K \left[ \frac{1-p}{2} y_1 + \frac{1-p}{2} y_3 + \frac{p}{2} y_4 \right] + A \sin(\omega t), \quad (20) \\ \dot{y}_3 &= \left[ 1 - \frac{K(1+p)}{2} \right] y_3 - y_3^3 \\ &\quad + K \left[ \frac{1-p}{2} y_1 + \frac{p}{2} y_2 + \frac{p}{2} y_4 \right] + A \sin(\omega t), \\ \dot{y}_4 &= \left[ 1 - \frac{K(p-2)}{2} \right] y_4 - y_4^3 \\ &\quad - K \left[ \frac{1-p}{2} y_1 + \frac{p}{2} y_2 + \frac{1-p}{2} y_3 \right] + A \sin(\omega t). \end{aligned}$$

Considering cluster A and cluster C have purely positive couplings, we define  $Y = (y_1 + y_3)/2$  and  $Z = (y_1 - y_3)/2$  as their average activity and synchronization error. Similarly, we define  $U = (y_2 + y_4)/2$  and  $W = (y_2 - y_4)/2$  as the average dynamics and synchronization error of cluster B and cluster D which are with purely negative couplings. Thus, Eq. (20) can be rewritten as

$$\dot{Y} = (1 - Kp - 3Z^2)Y - Y^3 + KpU + A \sin(\omega t), \quad (21)$$

$$\dot{Z} = (1 - K - 3Y^2)Z - Z^3, \quad (22)$$

$$\begin{aligned} \dot{U} &= (1 - Kp + K - 3W^2)U - U^3 - K(1-p)Y \\ &\quad + A \sin(\omega t), \quad (23) \end{aligned}$$

$$\dot{W} = (1 + K - 3U^2)W - W^3. \quad (24)$$

Accordingly, the average activity of Eq. (1) is given by

$$X = (1-p)Y + pU. \quad (25)$$

To obtain the analytical  $Y$  and  $U$ , we assume that the synchronization errors  $Z$  and  $W$  relax rapidly to their steady values, and hence may be adiabatically eliminated, i.e.,  $\dot{Z} = \dot{W} = 0$ . When  $\dot{W} = 0$ , Eq. (24) gives  $W = 0$  or  $W^2 = 1 + K - 3U^2$ . Since the two negatively coupled clusters with different initial conditions cannot achieve full synchronization, we substitute  $W^2 = 1 + K - 3U^2$  into Eq. (23), which yields

$$\dot{U} = -\alpha U + 8U^3 - K(1-p)Y + A \sin(\omega t), \quad (26)$$

where  $\alpha \equiv 2 + Kp + 2K > 0$ . As the two clusters with negative couplings only fluctuate around the fixed points [see Fig. 1(d)], we assume  $\dot{U} = 0$  and neglect the high-order term  $U^3$  in Eq. (26). Then the approximate solution of  $U$  is obtained as

$$U \approx \frac{K(p-1)}{\alpha} Y + \frac{A}{\alpha} \sin(\omega t). \quad (27)$$

Substituting Eq. (27) into Eq. (25) gives

$$X \approx \frac{(\alpha - pK)(1-p)}{\alpha} Y + \frac{pA}{\alpha} \sin(\omega t). \quad (28)$$

When  $\dot{Z} = 0$ , Eq. (22) implies that  $Z^2 = 1 - K - 3Y^2$  and  $Z = 0$ , which correspond to desynchronization and full synchronization between cluster A and cluster C, respectively. For the desynchronization case, substituting  $Z^2 = 1 - K - 3Y^2$  and Eq. (27) into Eq. (21), we obtain

$$\dot{Y} \approx \frac{-2\beta}{\alpha} Y + 8Y^3 + \frac{2\gamma A}{\alpha} \sin(\omega t), \quad (29)$$

where  $\beta \equiv 2 + 2Kp - K - 3K^2$  and  $\gamma \equiv 1 + Kp + K > 0$ . Similarly, the potential of Eq. (29) can be expressed as

$$V = \frac{\beta}{\alpha} Y^2 - 2Y^4 - \frac{2\gamma AY}{\alpha} \sin(\omega t). \quad (30)$$

Figure 4(e) shows the potential  $V$  at  $p = 0.3$  and  $K = 0.24$ . When  $t = 0$ ,  $V$  is M shaped with a single-well potential, and the potential barriers vanish when the signal  $2\gamma AY/\alpha \sin(\omega t)$  is at the maximum or minimum, e.g.,  $t = \pi/2\omega$ . Therefore,  $K_c = 0.24$  is the critical coupling strength beyond which the signal  $2\gamma AY/\alpha \sin(\omega t)$  is suprathreshold and cluster A and cluster C attain full synchronization. According to Eq. (12), this critical coupling strength satisfies

$$27\alpha\gamma^2 A^2 = \beta^3. \quad (31)$$

Figure 3(b) shows the relationship between  $K_c$  and  $p$  predicted by Eq. (31), which fits well to the boundary of region I.

The signal  $2\gamma AY \sin(\omega t)/\alpha$  is subthreshold for  $K < K_c$ , and the approximate solution of Eq. (29) can be obtained by linearization, which is given by

$$Y(t) \approx \frac{4A\beta\gamma}{\alpha^2\omega^2 + 4\beta^2} \sin(\omega t) - \frac{2A\alpha\gamma\omega}{\alpha^2\omega^2 + 4\beta^2} \cos(\omega t). \quad (32)$$

Substituting Eq. (32) into Eq. (28), we obtain the average activity as

$$X(t) \approx \frac{AM_1^{\frac{1}{2}}}{\alpha(\alpha^2\omega^2 + 4\beta^2)} \sin(\omega t + \phi_4), \quad (33)$$

where  $\phi_4$  is phase shift and  $M_1$  follows

$$M_1 \equiv [4\beta\gamma(1-p)(\alpha - pK) + p(\alpha^2\omega^2 + 4\beta^2)]^2 + 4\gamma^2\alpha^2\omega^2(1-p)^2(\alpha - pK)^2.$$

When  $K > K_c$ , cluster A and cluster C attain full synchronization. Using  $Z = 0$  and Eq. (27), Eq. (21) becomes

$$\dot{Y} \approx \frac{\theta}{\alpha}Y - Y^3 + \frac{2\gamma A}{\alpha} \sin(\omega t), \quad (34)$$

where  $\theta \equiv 2 + 2K - Kp - 3K^2p$ . Similarly, the potential of Eq. (34) can be written as

$$V = -\frac{\theta}{\alpha}Y^2 + 2Y^4 - \frac{2\gamma AY}{\alpha} \sin(\omega t), \quad (35)$$

which is a W-shaped potential with double well. Correspondingly, there also exists a critical coupling strength  $K_*$ , at which the potential barrier periodically disappears [see Fig. 4(f)]. Combing Eq. (12) and Eq. (35), the critical coupling strength  $K_*$  is governed by

$$27\alpha\gamma^2A^2 = \theta^3. \quad (36)$$

As shown in Fig. 3(b), the critical coupling strength  $K_*$  predicted by Eq. (36) is in good agreement with the boundary of region II.

The above analysis indicates that the signal  $2\gamma A \sin(\omega t)/\alpha$  remains subthreshold for Eq. (34) when  $K_c < K < K_*$ . In this coupling region, Eq. (34) can be solved by linearization, and the approximated solution is given by

$$Y(t) \approx \pm \sqrt{\frac{\theta}{\alpha}} + \frac{4A\gamma\theta}{\omega^2\alpha^2 + 4\theta^2} \sin(\omega t) - \frac{2A\alpha\gamma\omega}{\omega^2\alpha^2 + 4\theta^2} \cos(\omega t). \quad (37)$$

Substituting Eq. (37) into Eq. (33) gives

$$X(t) \approx \pm \sqrt{\frac{\theta}{\alpha}} \frac{(\alpha - pK)(1-p)}{\alpha} + \frac{AM_2^{\frac{1}{2}}}{\alpha(\alpha^2\omega^2 + 4\beta^2)} \sin(\omega t + \phi_5), \quad (38)$$

where  $\phi_5$  is the phase shift and  $M_2$  is

$$M_2 \equiv [4\theta\gamma(1-p)(\alpha - pK) + p(\alpha^2\omega^2 + 4\beta^2)]^2 + 4\gamma^2\alpha^2\omega^2(1-p)^2(\alpha - pK)^2.$$

Finally, when  $K > K_*$ , the signal  $2\gamma A \sin(\omega t)/\alpha$  is suprathreshold for Eq. (34). Accordingly, the amplitude of  $Y$  is determined by the cubic function,

$$Y^3 - \frac{\theta}{\alpha}Y - \frac{2\gamma A}{\alpha} = 0. \quad (39)$$

For  $\theta < 0$ , the amplitude of  $Y$  is given by

$$I_1 \equiv 2\sqrt{\frac{-\theta}{3\alpha}} \sinh \left[ \frac{1}{3} \operatorname{arsinh} \left( \frac{3\gamma A}{\theta} \sqrt{\frac{-3\alpha}{\theta}} \right) \right]. \quad (40)$$

For  $\theta > 0$ , the amplitude of  $Y$  is given by

$$I_2 \equiv 2\sqrt{\frac{\theta}{3\alpha}} \cosh \left[ \frac{1}{3} \operatorname{arcosh} \left( \frac{3\gamma A}{\theta} \sqrt{\frac{3\alpha}{\theta}} \right) \right]. \quad (41)$$

Assuming  $Y = I_{1,2} \sin(\omega t)$ , Eq. (28) becomes

$$X \approx \frac{(1-p)(\alpha - pK)I_{1,2} + pA}{\alpha} \sin(\omega t). \quad (42)$$

Combining Eqs. (33), (38), and (42), we can obtain the theoretical amplification for  $0 < p < 1$ :

$$G \approx \begin{cases} \frac{M_1^{\frac{1}{2}}}{\alpha(\alpha^2\omega^2 + 4\beta^2)}, & \text{if } K < K_c, \\ \frac{M_2^{\frac{1}{2}}}{\alpha(\alpha^2\omega^2 + 4\beta^2)}, & \text{if } K_c \leq K < K_*, \\ \frac{(1-p)(\alpha - pK)I_1 + pA}{A\alpha}, & \text{if } K_* \leq K, \theta < 0, \\ \frac{(1-p)(\alpha - pK)I_2 + pA}{A\alpha}, & \text{if } K_* \leq K, \theta > 0. \end{cases} \quad (43)$$

Figures 2(a) and 3(a) show the analytical amplifications of Eq. (43), which agree well with those obtained numerically from Eq. (1). Therefore, our reduced model (20) captures the macroscopic behavior of the original system (1), and confirms our hypothesis that three oscillation clusters support the enhanced signal amplification in a system of both positive and negative couplings.

## V. SUMMARY

In summary, we have analyzed the effects of positive and negative couplings in weak signal amplification, and found that the two types of couplings are complementary in their effects. The purely negative couplings prevent synchronization and cause a small average activity of the system, leading to a damped response to the weak external signal. The purely positive couplings act to pull the oscillators together to produce an amplified signal response, but such effect is limited in small coupling strength. However, when positive couplings coexist with negative couplings, the system can generate a significantly amplified signal response, showing resonancelike dependencies on both the coupling strength and the ratio between the two types of couplings. We further found that when the resonance occurs, the system splits into three oscillation clusters—two negatively coupled clusters fluctuate around two fixed points and one positively coupled cluster oscillates between the two fixed points. Using reduced models based on oscillation clusters, we analyze the response of the system for cases of purely positive couplings, purely negative couplings, and mixed positive and negative couplings, which predict well the numerical observations. These findings highlight the complementary effect of positive and negative couplings on weak signal amplification. We note that the phenomenon is obtained for the globally coupling scheme (1). As mentioned earlier, the heterogeneous interaction

topologies are more commonly observed in neural networks; a new study about the interplay of network structure and mixed couplings on signal amplification is warranted for future work.

#### ACKNOWLEDGMENTS

X.L. was supported by the National Natural Science Foundation of China under Grants No. 11305078 and No. 61877030.

- 
- [1] R. L. Badzey and P. Mohanty, *Nature (London)* **437**, 995 (2005).
  - [2] A. Samardak, A. Nogaret, N. B. Janson, A. G. Balanov, I. Farrer, and D. A. Ritchie, *Phys. Rev. Lett.* **102**, 226802 (2009).
  - [3] R. B. Karabalin, Ron Lifshitz, M. C. Cross, M. H. Matheny, S. C. Masmanidis, and M. L. Roukes, *Phys. Rev. Lett.* **106**, 094102 (2011).
  - [4] P. Hänggi, *Chem. Phys. Chem.* **3**, 285 (2002).
  - [5] X. Han, Y. Zhang, Q. Bi, and J. Kurths, *Chaos* **28**, 043111 (2018).
  - [6] B. Lindner, J. Garcia-Ojalvo, A. Neiman, and L. Schimansky-Geier, *Phys. Rep.* **392**, 321 (2004).
  - [7] F. Sagués, J. M. Sancho, and J. García-Ojalvo, *Rev. Mod. Phys.* **79**, 829 (2007).
  - [8] M. D. McDonnell and L. M. Ward, *Nat. Rev. Neurosci.* **12**, 415 (2011).
  - [9] F. Moss, D. Pierson, and D. O’Gorman, *Internat. J. Bifur. Chaos* **04**, 1383 (1994).
  - [10] L. Gammaitoni, P. Hänggi, P. Jung, and F. Marchesoni, *Rev. Mod. Phys.* **70**, 223 (1998).
  - [11] J. F. Lindner, B. K. Meadows, W. L. Ditto, M. E. Inchiosa, and A. R. Bulsara, *Phys. Rev. Lett.* **75**, 3 (1995).
  - [12] C. Zhou, J. Kurths, and B. Hu, *Phys. Rev. Lett.* **87**, 098101 (2001).
  - [13] A. Pikovsky, A. Zaikin, and M. A. de la Casa, *Phys. Rev. Lett.* **88**, 050601 (2002).
  - [14] C. J. Tessone, C. R. Mirasso, R. Toral, and J. D. Gunton, *Phys. Rev. Lett.* **97**, 194101 (2006).
  - [15] M. Gassel, E. Glatt, and F. Kaiser, *Phys. Rev. E* **76**, 016203 (2007).
  - [16] T. Perez, C. R. Mirasso, R. Toral, and J. D. Gunton, *Phil. Trans. R. Soc. A* **368**, 5619 (2010).
  - [17] J. F. Mejias and A. Longtin, *Phys. Rev. Lett.* **108**, 228102 (2012).
  - [18] K. Padmanabhan and N. N. Urban, *Nat. Neurosci.* **13**, 1276 (2010).
  - [19] E. Bullmore and O. Sporns, *Nat. Rev. Neurosci.* **10**, 186 (2009).
  - [20] C. Gu, J. Wang, and Z. Liu, *Phys. Rev. E* **80**, 030904(R) (2009).
  - [21] J. Zhou, Y. Zhou, and Z. Liu, *Phys. Rev. E* **83**, 046107 (2011).
  - [22] C. Zhou, A. E. Motter, and J. Kurths, *Phys. Rev. Lett.* **96**, 034101 (2006).
  - [23] X. Zhang, S. Boccaletti, S. Guan, and Z. Liu, *Phys. Rev. Lett.* **114**, 038701 (2015).
  - [24] Z. Gao, B. Hu, and G. Hu, *Phys. Rev. E* **65**, 016209 (2001).
  - [25] M. Perc, *Phys. Rev. E* **76**, 066203 (2007).
  - [26] J. A. Acebrón, S. Lozano, and A. Arenas, *Phys. Rev. Lett.* **99**, 128701 (2007).
  - [27] Z. Liu and T. Munakata, *Phys. Rev. E* **78**, 046111 (2008).
  - [28] L. Wu, S. Zhu, and X. Luo, *Chaos* **20**, 033113 (2010).
  - [29] T. Vaz Martins, V. N. Livina, A. P. Majtey, and R. Toral, *Phys. Rev. E* **81**, 041103 (2010).
  - [30] X. Liang, L. Zhao, and Z. Liu, *Chaos* **22**, 023128 (2012).
  - [31] C. Liu and X. Liang, *Phys. Rev. E* **100**, 032206 (2019).
  - [32] R. A. Stefanescu and V. K. Jirsa, *PLoS Comput. Biol.* **4**, e1000219 (2008).
  - [33] X. Liang, M. Tang, M. Dhamala, and Z. Liu, *Phys. Rev. E* **80**, 066202 (2009).
  - [34] E. Fino and R. Yuste, *Neuron* **69**, 1188 (2011).
  - [35] I. Leyva, I. Sendiña-Nadal, J. A. Almendral, and M. A. F. Sanjuán, *Phys. Rev. E* **74**, 056112 (2006).
  - [36] H. Hong and S. H. Strogatz, *Phys. Rev. Lett.* **106**, 054102 (2011).
  - [37] X. Zhang, Z. Ruan, and Z. Liu, *Chaos* **23**, 033135 (2013).
  - [38] X. Zhang, S. Guan, Y. Zou, X. Chen, and Z. Liu, *Europhys. Lett.* **113**, 28005 (2016).
  - [39] G. Balázsi, A. H. Cornell-Bell, and F. Moss, *Chaos* **13**, 515 (2003).
  - [40] X. Chen and R. Dzakpasu, *Phys. Rev. E* **82**, 031907 (2010).
  - [41] G. G. Turrigiano and S. B. Nelson, *Nat. Rev. Neurosci.* **5**, 97 (2004).